Plasma-enhanced atomic layer deposition of silicon nitride thin films with different substrate biasing using Diiodosilane precursor

Mohammed Zeghouane, Gauthier Lefevre, Sébastien Labau, Mohammed-Bilal Hachemi, Franck Bassani, Bassem Salem

Materials Science in Semiconductor Processing 184 (2024) 108851

Contents lists available at ScienceDirect

Materials Science in Semiconductor Processing

journal homepage: www.elsevier.com/locate/mssp

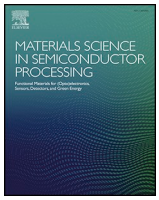

Plasma-enhanced atomic layer deposition of silicon nitride thin films with different substrate biasing using Diiodosilane precursor

Mohammed Zeghouane, Gauthier Lefevre, Sebastien Labau, Mohammed-Bilal Hachemi, Franck Bassani, Bassem Salem *

Univ. Grenoble Alpes, CNRS, CEA/LETI Minatec, Grenoble INP, LTM, 38054, Grenoble, France

ARTICLE INFO

Keywords:
Plasma-enhanced atomic layer deposition
Diiodosilane
Silicon nitride
Substrate biasing

ABSTRACT

In this work, we report on Plasma-Enhanced Atomic Layer Deposition (PE-ALD) of SiN_x films using Diiodosilane (DIS) precursor and N_2-H_2 plasma. Systematic studies as a function of DIS dosing time, plasma duration, plasma composition and deposition temperature are investigated. The material properties have been studied using X-ray photoelectron spectroscopy (XPS), X-Ray Reflectometry (XRR), Atomic Force Microscopy (AFM) and High-Resolution Transmission Electron Microscopy (HR-TEM). The optimal deposition parameters for achieving high-quality SiN_x with a high growth per cycle (GPC) are first determined. We show that DIS offers a wide temperature window for SiN_x deposition starting from 110 °C up to 300 °C, paving the way for a large choice of SiN-based applications. The impact of substrate biasing on SiN_x film deposition and properties is also investigated. We show that high ion energies during the nitridation step can cause surface damage and void formation, thus affecting the SiN_x quality. Overall, these results highlight the importance of this novel precursor for growing SiN_x using PE-ALD and the possible swapping of the material properties by fine control of the substrate biasing, which can help to go far beyond the existing SiN_x limitations.

1. Introduction

Silicon nitride is a widely studied material due to its very extensive range of applications. e. g. in memory, as a floating gate, and in transistors, as a nitride spacer [1–5]. However, the requirement for controlling the film properties with a good coverage over the nanoscale is becoming more stringent. Atomic Layer deposition (ALD) has gained importance due to the ability to grow these films with good step coverage with excellent uniformity and conformal coatings on high-aspect-ratio structures. The ALD also enables to grow thin films with a precise control of the thickness even over complex structures, due to the layer-by-layer growth in a self-limiting manner by active sites [6, 7]. There are currently many reports on ALD-SiN_x using thermally activated reactions. Most of the current works have been focused on chlorosilanes (Si-Cl) based precursors in combination with co-reactants such as NH_3 or N_2H_4. However, processing with chlorosilanes requires high activation temperatures or high concentrations to ensure a sufficient surface reaction and can lead to the production of corrosive vapor HCl during the process [7–12]. To date, however, in the semiconductor industry, there remains a need for high-quality SiN_x films deposited at low temperatures. This is why Plasma Enhanced ALD (PE-ALD), where plasmas can be employed as co-reactant to increase the core-actant's reactivity, can be more attractive for growing thin films at lower temperatures, giving the process more flexibility [13]. However, despite its high reactivity, long plasma times are needed to avoid impurity incorporation in the growing films, and thus chlorine-free precursors are highly desired. For this reason, PE-ALD SiN_x thin films using chlorine-free precursors and N_2 plasma or NH_3 plasma as co-reactant have been developed and various precursors have been studied [14–18]. On the other hand, the substrate biasing technique in the PE-ALD process, where ion energies can be varied by tuning the sample's bias voltage, has shown potential advantages allowing for improvement in the material properties [19–24]. However, to our knowledge, no studies to date have been conducted on PE-ALD SiN_x thin films using substrate biasing.

This paper reports on PE-ALD SiNx deposition using a Diiodosilane precursor, where silicon halide precursor comprises two iodine (H_2I_2Si), and N_2-H_2 reactants. The DIS precursor gives the added benefits for growing SiN_x at low temperatures due to its low bond dissociation energy (Si-I: 284 kJ/mol) [13], allowing an easy interaction with

* Corresponding author. Univ. Grenoble Alpes CNRS, CEA/LETI Minatec, LTM, 38054, Grenoble, France.
E-mail address: Bassem.salem@cea.fr (B. Salem).

https://doi.org/10.1016/j.mssp.2024.108851
Received 16 May 2024; Received in revised form 25 July 2024; Accepted 24 August 2024
Available online 30 August 2024

high-density dangling bonds' surfaces. The optimal growth parameters for achieving SiN_x deposition with a high growth per cycle (GPC) will first be presented. A first evaluation of the substrate biasing at 300 °C on SiNx films deposition and properties will be discussed.

2. Experimental details

SiN_x thin films were deposited on Si substrates using Plasma-Enhanced Atomic Layer Deposition (PE-ALD) within an Oxford Instruments FlexAL reactor. This reactor is equipped with a remote inductively coupled (ICP) plasma source, operated at 300 W of radio frequency power, for providing species needed for nitridation. A second additional power supply is connected to the substrate holder and allows to generate an RF-biased substrate up to 100 W, enabling to change the film properties. Diiodosilane (DIS) synthesized and provided by Air Liquide Advanced Materials., was used as a Si precursor and held at a bubbler temperature of 50 °C. DIS vapor was driven into the reaction chamber using Argon (Ar, 99,999 %) as a carrier gas. Nitrogen (N_2, 99,999 %) gas was used as a precursor for nitrogen source. Additional hydrogen (H_2, 99,999 %) gas was added into the reaction chamber during the nitridation step and Ar was used as purging gas. The n-doped Si (001) substrates were cleaned with hydrochloric acid (HCl) for 3 min, rinsed in deionized water and dried with N_2. Fig. 1(a) shows the step sequences of one cycle of SiN deposition used in this work. First, DIS was injected into the reaction chamber carried by 150 sccm of Ar gas. Then, the chamber was purged with 100 sccm flow of Ar gas for 3 s to remove the excess of DIS and the products reaction. During the second half of the cycle, a plasma of ionized N_2 and H_2 was created to provide ions and radicals needed for nitridation (without Ar carrier gas). Finally, the chamber was purged out with 100 sccm flow of Ar gas. Here, the purge time of 3 s was fixed based on the saturation curves for precursor dosage and plasma exposure obtained during the process development of previous works [19]. The surface chemical reactions of SiN_x deposition are illustrated in Fig. 1(b). Briefly summarized, the hydrogen-terminated starting surface is exposed to Diiodosilane that reacts with the surface in a self-limiting reaction. Once the chamber is purged to remove excess precursor and by-products, the second co-reactant, nitrogen is introduced to react and form one monolayer of SiN_x. This allows the process to be cycled and control precisely the growth thickness. The growth was monitored in situ by multi-wavelength ellipsometry. The measured thicknesses were obtained by fitting parameters using a nonlinear regression algorithm (Marquardt–Levenberg) on Film Sense Software. Fig. 2 shows an example of the variation of the thickness with the different pulsing sequences of one SiN_x cycle determined by in-situ ellipsometry.

The final thickness and density were measured by XRR using a Bruker D8 Advance diffractometer with Cu Kα1 radiation. The structural properties of the growing SiN_x films were investigated using High-

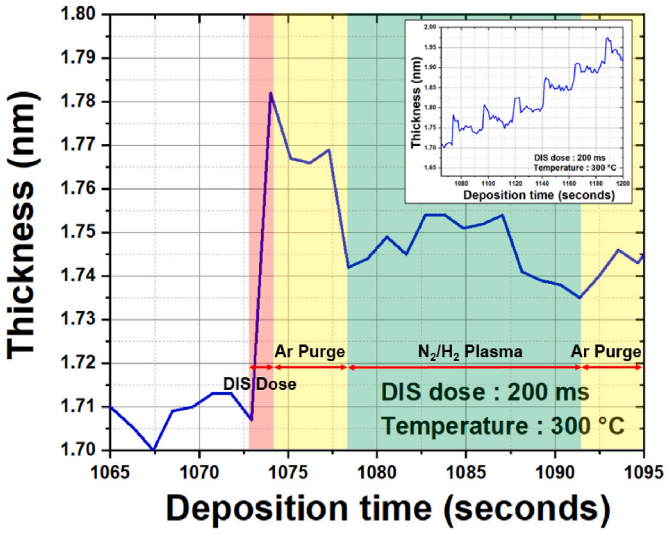

Fig. 2. SiN thickness determined by ellipsometry as a function of time, example of one PE-ALD cycle, including DIS injection (200 ms, red region), N_2:H_2 plasma (15 s, green region), and Ar purges (3 s, yellow regions). The inset shows the in-situ measurement of SiN thickness from ellipsometry for a large window of deposition time.

Resolution Transmission Electron Microscopy after focused ion beam (FIB, Helios Nanolab 450S from FEI) preparation along the [110] zone axis. Surface morphology of the layers was investigated using tapping mode Atomic Force Microscopy (AFM) on a Bruker Dimension Icon system. The chemical composition and spatial distribution of elements were measured by X-ray photoelectron spectroscopy (XPS) on a customized parallel angle resolved (pARXPS) Theta 300 from Thermo Fisher Scientific. The samples were irradiated with a beam size of 400 μm of monochromatized Al–Kα source (1486.6 eV). The ejected electrons were collected, with an incident angle ranging from 23.75° to 76.25° with regard to the sample's surface normal, by a hemispherical analyzer at 100 eV constant pass energy. This allows us to have resolved peaks at all angles in an acceptable acquisition time. Indeed, parallel angular XPS analysis collects data on all angles and then divides the signal according to the number of desired angles (6 angles in our case). This means that the signal is less resolved for each individual angle (especially and higher incident angles). Therefore, a pass energy of 100eV is the best compromise for good accuracy and optimization of the experiment's duration. The energy scale was calibrated using the surface C 1s peak, from the carbon surface contamination, at 284.8 eV. The XPS data were fitted using the ThermoScientific provided software, Avantage 5.902. We also used the built-in reference library to constrain the peaks

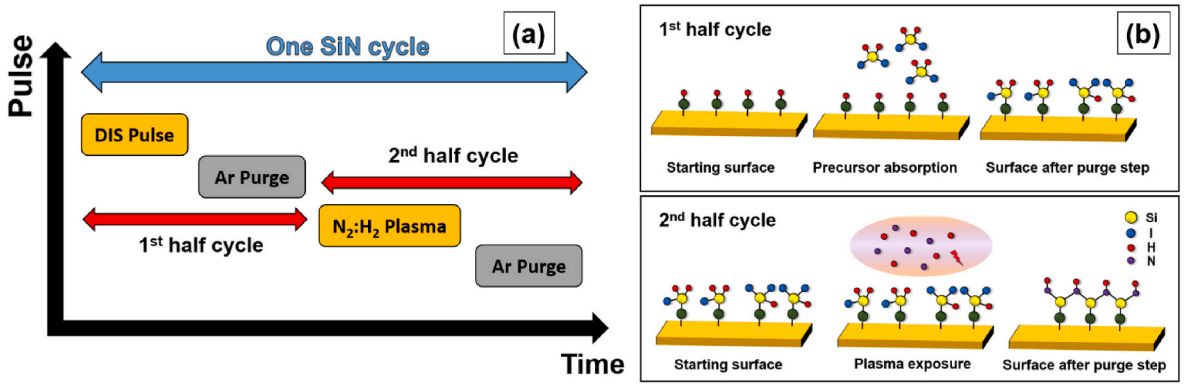

Fig. 1. (a) Schematic of the pulsing sequences of one SiN cycle. **(b)** Schematic of one cycle of typical PE-ALD process for SiN deposition using DIS and N_2-H_2 as precursors.

obtained. Indeed, all peaks fitted at a given binding energy were constrained to have the same binding energy, same full width at half maximum (FWHM), and same Tail mix height and exponent for all samples. The baseline is placed automatically in a given spectra using a built-in "smart" method. The number of peaks is determined both physically and according to the shape of the recorded peak to "fit" it properly.

3. Results and discussion

First, the growth per cycle (GPC) of SiN_x is measured as a function of DIS exposure time to confirm if DIS is an appropriate PE-ALD precursor. The films were deposited at 300 °C and the plasma power was set at 300 W. The DIS purge time, N_2:H_2 plasma duration and plasma purge time were fixed to 3 s, 15 s and 3 s, respectively. The N_2:H_2 fluxes were 20:10 sccm and the total cycles were 100 c. Fig. 3(a) shows the GPC of SiN_x deposition as function of DIS exposure time and confirms the saturation-like behavior. The GPC slightly increases from 0.33 to 0.4 Å/cycle when the DIS injection time increases from 50 to 300 ms. Several studies dealing with SiN_x deposition by PE-ALD using different Si-containing precursors have shown similar curves of the GPC as a function of precursor dosing time [14,15]. Such quick saturation as a function of dosing time suggests that the precursor quickly occupies the free reactive surface sites. However, the GPC as a function of N_2:H_2 plasma exposure time shows a soft-like saturation behavior as can be seen in Fig. 3(b). Similar growth rates were observed using a pure N_2 or a mixture of N_2:H_2 plasma [25,26]. Here, the presence of some fraction of hydrogen in plasma increases approximately three times the growth rate as illustrated in Fig. 3(c). C. K. Ande et al. have conducted an in-depth study using the first principal calculation showing the important role of the co-reactants' composition, comparing N_2 plasma, N_2−H_2 plasma, or NH_3 plasma [26]. Indeed, the co-reactants help to remove ligands from the precursor after the first half cycle (as depicted in Fig. 1(b)), thereby generating reactive surface sites thereafter. This facilitates the surface reaction of precursors, leading to optimal growth per cycle. Based on these experiments, the standard PE-ALD process for SiN_x deposition using DIS was defined and given in Table 1. These process parameters are chosen according to the GPC saturation at a particular value. On the other hand, it can be observed from Fig. 3(b) that the growth of SiN_x can be closer to the saturation for a longer plasma N_2-H_2 exposure time, higher or equal to 30 s. This implies a longer cycle time which requires several hours to grow a thick SiN_x film. To this end, the plasma exposure

Table 1
Standard and optimal growth parameters for SiN_x deposition developed in this work using DIS and N_2-H_2 plasma.

Experiment parameter (unit)	Value
Precursors dose time (ms)	200
Precursor purge time (s)	3
Plasma exposure time (s)	15
Plasma pure time (s)	3
Bubbler temperature (°C)	50
H_2/N_2 ratio	0.5

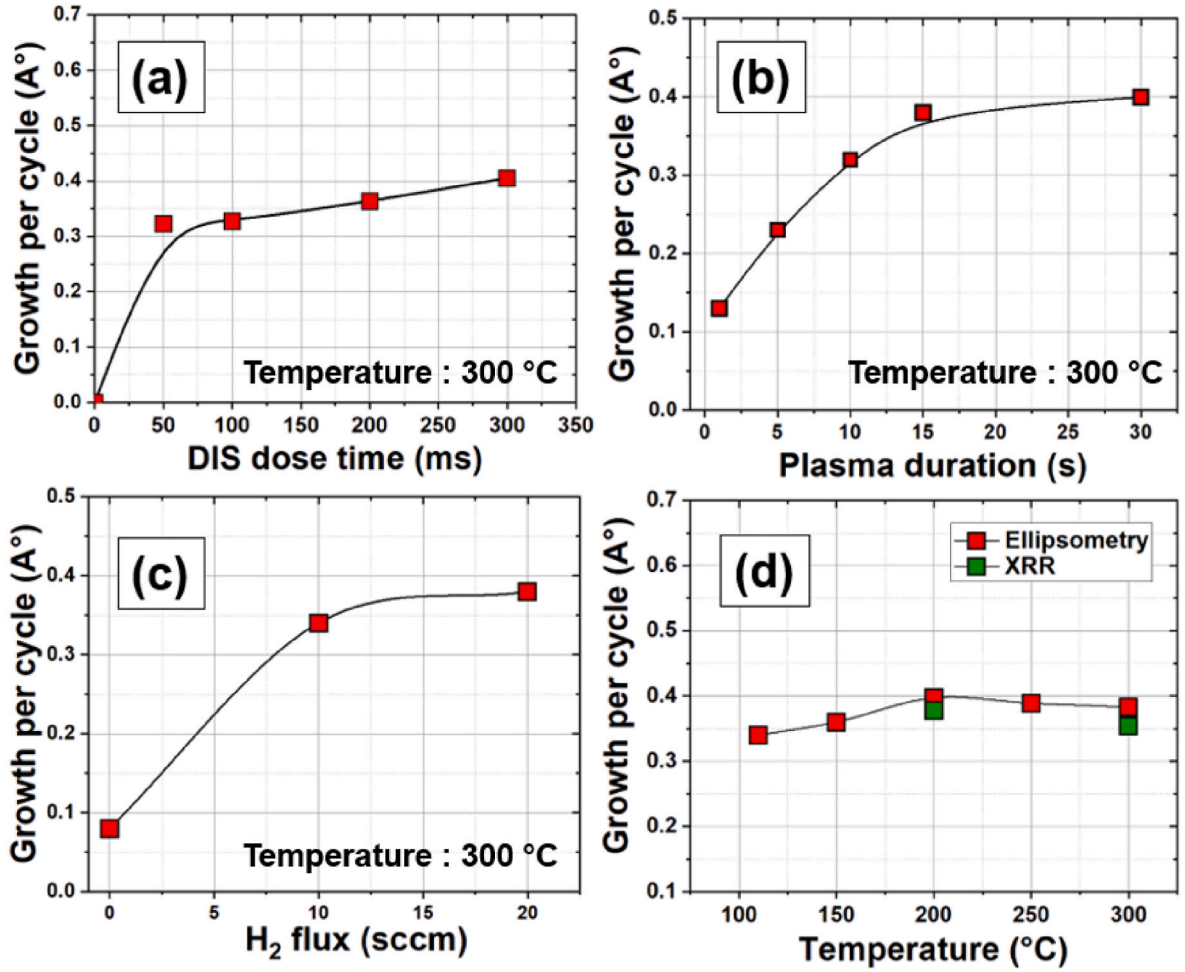

Fig. 3. Growth per cycle (GPC) obtained from ellipsometry measurements as a function of **(a)** DIS dose time, **(b)** plasma duration and **(c)** plasma composition with hydrogen **(d)** deposition temperature. The DIS and plasma purges time were fixed at 3 s. The lines are guide for the eye only.

time was chosen to be set at 15 s for the standard process condition.

The use of DIS as a silicon precursor in combination with a plasma-enhanced process relates principally on the low temperature deposition capability of SiN_x films. This is why the temperature dependence of SiN_x deposition has also been studied. The DIS injection and plasma exposure were kept at 200 ms and 15 s, respectively. Fig. 3(d) shows the GPC of SiN_x growth at different deposition temperatures: 110 °C, 150 °C, 200 °C, 250 °C and 300 °C. The GPC is nearly constant, around 0.36 ± 0.04 Å, over the process temperatures range from 110 °C to 300 °C. This suggests that such temperatures lie within the PE-ALD window of DIS, i.e. this temperature range can therefore be considered to be high enough for avoiding precursors condensation on the substrate surface, and low enough to avoid Si-N decomposition and/or precursors desorption. Of course, this provides the advantage of DIS for growing SiN_x with a large choice of deposition temperatures, giving the material more flexibility. In fact, there is no significant difference in structural and chemical properties of SiN_x as a function of the deposition temperature. More detailed structural and physico-chemical characterizations by HR-TEM, AFM, EDX and XPS of SiN_x at different deposition temperatures can be found in the Supporting Information. Here, we have chosen to present only the results of characterization on SiN_x obtained at 300 °C. The HR-TEM image, after FIB preparation, of 5 nm-thick PE-ALD SiN_x, shown in Fig. 4(a), confirms the amorphous quality of SiN_x keeping a good interface quality with the substrate and without any interfacial layer formation even at 300 °C and/or after plasma exposure. The smooth surface of the growing SiN_x film is confirmed by AFM, as shown in Fig. 4 (b), with a root-mean-square (RMS) roughness equal to 0.19 nm. It is important to note that the surface roughness remains relatively low, around 0.15–0.19 nm, even on 30 nm-thick SiN_x layers. The XPS core level of Si 2p and N 1s peaks recorded for SiN film deposited at 300 °C are shown in Fig. 4(c–d). For Si 2p, two components are identified at 101.5 and 102.9 eV corresponding to Si−N bonds and Si−O bonds, respectively. The N 1s spectrum at 397.3 eV is attributed to N-Si bonds consistent with the reported values of Si_3N_4 grown by ALD and PE-CVD

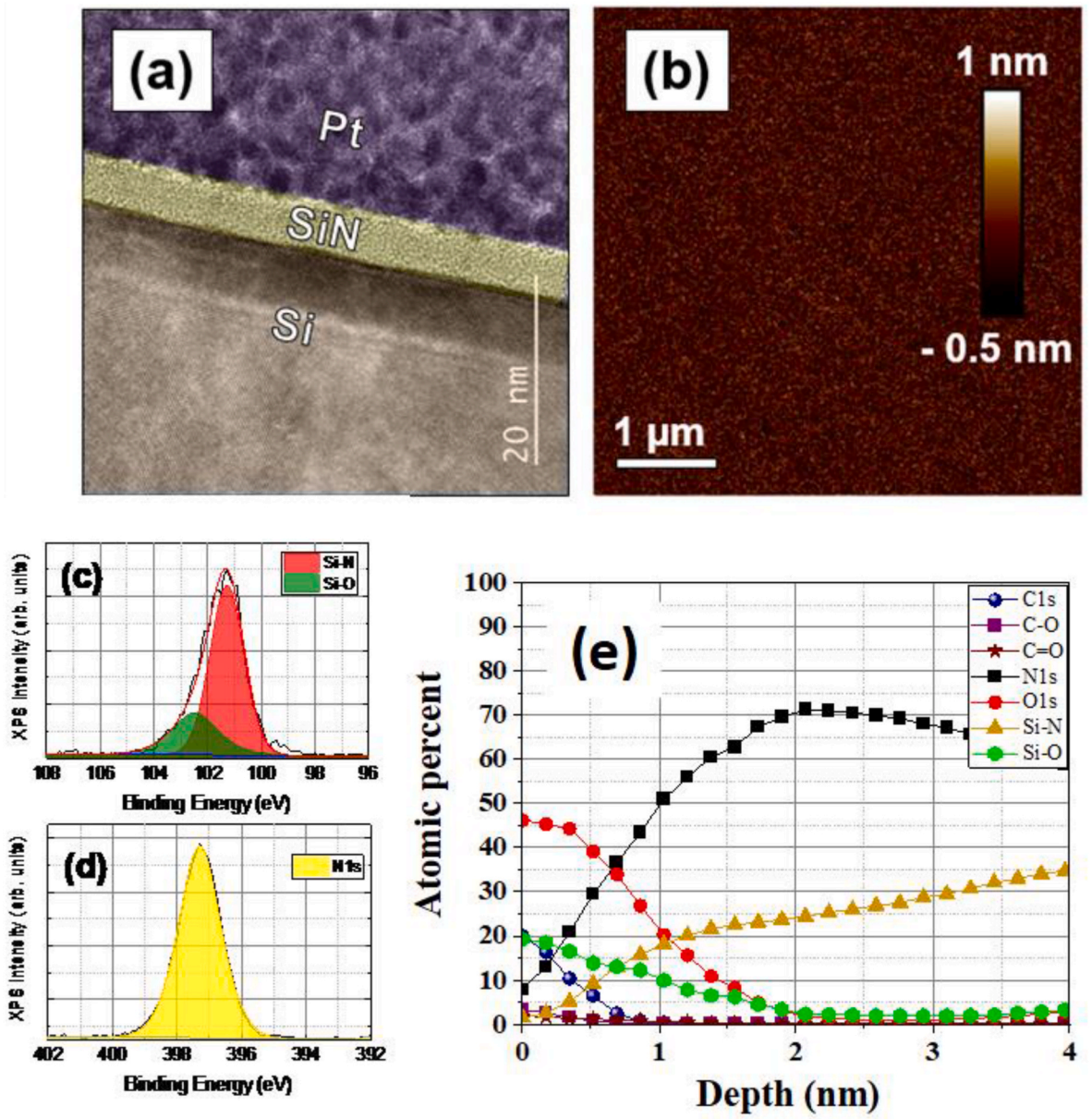

Fig. 4. Structural and chemical properties of SiN_x thin film grown at 300 °C with 100 cycles **(a)** HR-TEM image taken after a FIB preparation showing the amorphous quality of the grown SiN_x film on Si substrate. (b) AFM image showing the smooth surface of the SiN_x film with an RMS = 0.19 nm. XPS spectra with an incident angle of 23.75°of (c) Si 2p and (d) N 1s measured from the grown SiN film and (e) is the XPS depth profile showing the chemical distribution of SiN_x elements.

[27]. More interestingly, no iodine atoms have been detected by XPS. The pARXPS depth profiling is depicted in Fig. 4(e) showing the chemical distribution of SiN-containing elements over the first 4 nm in depth. The observed high O and C concentrations at the film surface is due to surface contamination and SiN_x oxidation post-deposition. The approximately constant Si and N atomic contents in-depth indicate uniform film stoichiometry with an N/Si ratio of 1.27, closely matching stoichiometric Si_3N_4, throughout the entire film thickness. A slight variation in this ratio was noticed with the growth temperature as shown in the supporting information. The N/Si ratio decreases from 1.27 to 0.98 when the temperature decreases from 300 °C to 110 °C (see Supporting Information Table S1), due to the thermally enhanced growth reactions. Finally, the growing SiN film at 300 °C has a bulk film density of 3.17 g/cm^3, measured by XRR, which is comparable to the reported density of Si_3N_4 (2.30–3.25 g/cm^3) [13]. Overall, it can be concluded that DIS brings practical benefits for growing smooth and stoichiometric SiN_x with a large choice of deposition temperatures, paving the way for various applications. However, the need for hydrogen during plasma nitridation to enhance the growth rate, can lead to the incorporation of hydrogen in SiN bulk, thereby altering the overall film quality. It is known that the Si-H/N-H ratio is a predictor of the refractive index (RI) and film stress of growing SiN films. The hydrogen incorporation can be reduced by further optimizing the growth conditions.

Now, after finding the ALD process window for SiN_x using DIS, the material properties, including density, impurities, stoichiometry, and defects, can be further modified/optimized by using substrate biasing. Varying the bias voltage at the substrate holder can modify surface reactions and adatom diffusion and therefore the film properties. The optimum deposition condition using bias must be carefully evaluated to improve the film quality because higher ions energy can lead to surface implantation, roughness and sputtering. To do this, we studied the impact of substrate biasing on SiN_x growth while fixing the growth temperature at 300 °C, DIS injection at 200 ms, and the N_2:H_2 plasma duration at 15 s. The N_2 and H_2 fluxes were kept at 20 sccm and 10 sccm, respectively and the total cycle was 250 c. Fig. 5(a) shows the variation of the GPC of SiN_x deposition, obtained by in-situ ellipsometry, as a function of substrate bias, per power unit. The equivalent bias voltages are given in Supporting Information (Fig. S5). Clearly, the GPC is strongly influenced by bias power and, two different trends are highlighted. At low biases, ≤10 W, corresponding to a lower ion energy, the GPC remains relatively stable around 0.385 ± 0.015 Å/cycle. Hoverer, at higher biases, >10 W, a strong decrease in GPC is clearly observed. This trend was already observed in previous works dealing with AlN [19], HfO_2 [24] and TiO_2 [22]. The authors assume that such a decrease in GPC at high ion energy may arise from the removal of reactive sites and/or surface damage.

The change in the growth rate of SiN_x films by applying substrate biasing typically indicates an evolution of the microstructure with the assistance of energetic ions during the nitridation step. Fig. 5(b) shows the effect of the substrate bias on SiN_x films' density. Compared to the SiN_x films deposited without substrate biasing, the SiN density decreases and reaches the minimum values of 2.8 ± 0.05 g/cm^3 when increasing the bias voltage until 10 W and starts to slightly increase around 2.98 g/cm^3 at 40 W. Such an increase in densities at high bias voltages may indicate a deterioration in the film's morphology under intense ion bombardment, leading to less dense films. A similar effect was also observed for HfO_2 deposited in the FlexAL system and the authors suggest the formation of void-rich microstructures due to the energetic ions bombardment [24]. This variation of SiN_x film's morphology with substrate biasing is also evident in the surface roughness measured by AFM as shown in Fig. 6. The SiN_x films deposited with 0, 5, 10 and, 20 W of bias show smooth surfaces and the RMS decreases slightly from 0.19 to 0.13 nm when increasing the bias from 0 W to 20 W. However, for higher bias (≥40 W) random nano-islands are formed which induces a significant increase of the roughness. In fact, the evolution of the surface roughness with the bias depends also on the film thickness. It has been shown that thin films are amorphous at the initial growth stage and then crystallize when the film thickness exceeds a critical value [28]. Here, we have shown the GPC decreases with bias, resulting in a decrease in total thickness. Some authors have shown the same trend of roughness with increasing the bias during the growth of HfO_2 and AlN using PE-ALD FlexAL reactor [19,24]. Films deposited with moderate biases are smoother compared to films deposited without bias. V. Beladiya et al. explain that smoother surfaces at moderate bias can result from the increased mobility of ad-species induced by energetic ions, improving coalescence at the grain boundaries [24]. However, intense ion bombardment at higher bias results in a significant increase in surface roughness due to strong surface damage and/or void formation.

In order to better understand the effect of substrate biasing on SiN_x films' properties, we performed XPS measurements on these samples. The XPS core level of Si 2p and N 1s peaks recorded for SiN_x films deposited at different biases, and acquired at 23.75°, are shown in Fig. 7. Whatever the substrate biasing, the N 1s peak position remains relatively constant around 397.3 eV. However, we can notice a slight variation in Si 2p peaks intensity with the bias, more specifically, the intensity of the peak position at 102.9 eV, corresponding to Si-O bonds, which increases with increasing bias. The appearance of Si-Si bonds at 98.7 eV for the SiN_x film grown with a higher bias of 40 W can be attributed to Si-Si bonds from the silicon substrate due to the lower SiN_x thickness at such substrate biasing. The impurity content and the chemical composition of SiN_x films deposited at different biases and determined from XPS analysis are listed in Table 2. The C content decreased slightly until 4.7 % when a bias power of 40 W was applied. This is due to the enhanced impurities removal with energetic ions as discussed in previous studies. The N/Si ratio decreases also with substrate biasing which can be related to a lower Si nitridation and/or N

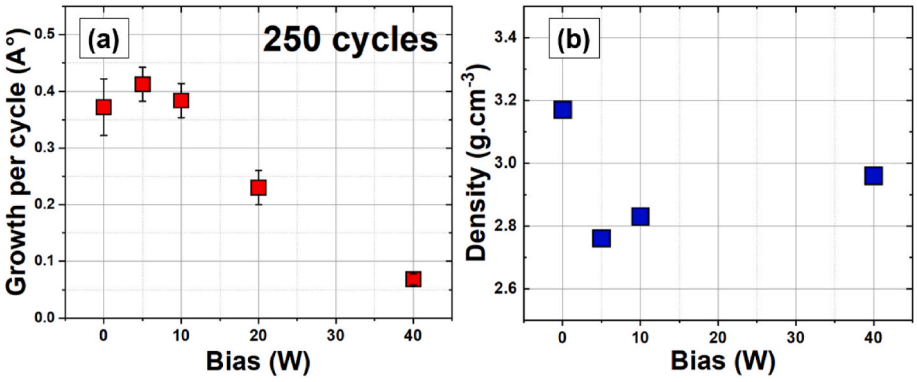

Fig. 5. **(a)** Growth rate Per Cycle (GPC) of SiN_x deposition at 300 °C as a function of bias measured by in situ ellipsometry. **(b)** Density variation of SiN films with bias obtained by XRR simulation. The total cycle is 250.

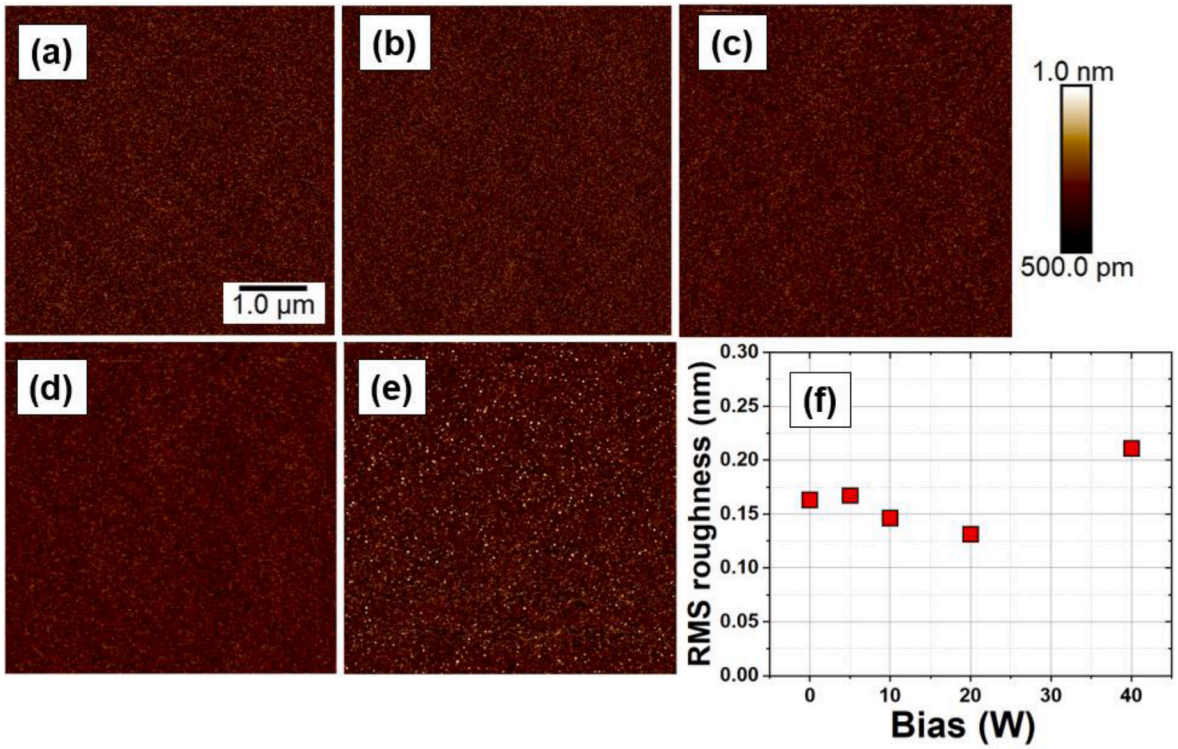

Fig. 6. AFM images of SiN_x surfaces grown at 300 °C **(a)** without bias and with different applied biases **(b)** 5 W, **(c)** 10 W, **(d)** 20 W and **(e)** 40 W. **(f)** RMS surface roughness of SiN as a function of substrate bias.

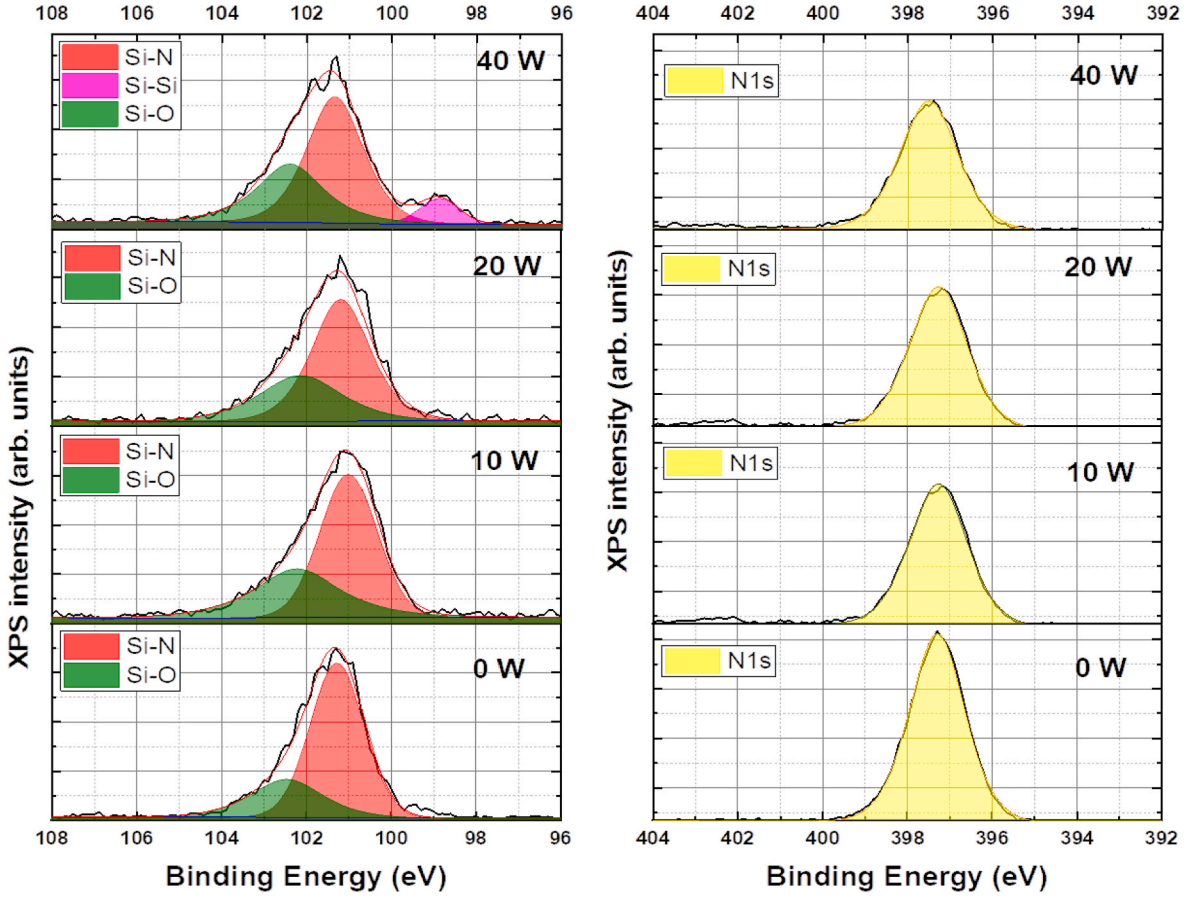

Fig. 7. XPS spectra with an incident angle of 23.75° of Si2p and N1s recorded from SiN_x films grown at different substrate biasing.

Table 2
Atomic concentrations of SiN_x thin films deposited with 250 cycles at different bias and determined by XPS with an incident angle of 23.75°

Bias power (W)	Si (%)	N (%)	O (%)	C (%)	N/Si
0	33.3 ± 1.2	42.5 ± 0.8	18.1 ± 0.7	5.8 ± 0.7	1.27
5	34.6 ± 1.2	37.6 ± 0.8	21.6 ± 0.5	6.0 ± 0.3	1.09
10	32.3 ± 0.5	36.9 ± 0.4	25.7 ± 0.4	5.8 ± 0.5	1.14
20	31.8 ± 0.7	34.8 ± 0.6	28.0 ± 0.7	5.6 ± 0.9	1.09
40	31.3 ± 1.0	33.4 ± 1.2	29.6 ± 0.8	4.7 ± 0.7	1.06

desorption, as the N content reduces. On the other hand, SiN_x films become oxygen-rich when increasing the bias, i.e., the incorporation of oxygen increases with the bias. As discussed in previous papers, the surface damage caused by high ion bombardment may induce voids formation and absorption of moisture, fostering SiN oxidation [24,29,30]. Overall, these results demonstrate the effect of substrate biasing on SiN_x properties and reveal that a substrate bias of 5 W generates sufficiently energetic ions to cause surface damage, unlike what has been observed for AlN [19]. It is therefore important to optimize the process with lower ion energies (moderate bias power <5 W) to improve the Si nitridation step with less damage and impurity incorporation, thus, to obtain SiN_x with improved properties, surpassing those of existing SiN_x materials.

4. Conclusion

In conclusion, PE-ALD SiN_x films close to the stoichiometric Si_3N_4 were deposited using Diiodosilane (DIS) precursor. We showed that DIS is a suitable precursor for growing SiN films over a wide temperature range, from 110 °C to 300 °C, while maintaining the same GPC and film properties. It was revealed that hydrogen during the plasma nitridation step is needed to achieve a high SiN growth rate, however, its incorporation in SiNx material could be reduced by optimizing further the growth condition. The plasma duration of 15 s was found to be high enough for nitridation. On the other hand, we have studied the impact of substrate biasing on SiN film properties. We have shown that GPC, density, roughness and chemical composition were heavily affected by the bias applied to the substrate. The bias powers explored in this work, from 5 to 40 W, were high enough to provoke surface damage, resulting in SiN_x degradation. However, it will be interesting to use moderate biases, lower than 5 W, to improve SiN_x film purity and properties. Overall, the PE-ALD process window for SiN_x deposition using DIS was calibrated, and DIS appears to be a relevant promising precursor for future SiN film-based devices.

CRediT authorship contribution statement

Mohammed Zeghouane: Writing – original draft, Methodology, Investigation, Formal analysis, Data curation, Conceptualization. **Gauthier Lefevre:** Writing – review & editing, Investigation, Formal analysis. **Sebastien Labau:** Writing – review & editing, Investigation, Formal analysis. **Mohammed-Bilal Hachemi:** Writing – review & editing, Formal analysis. **Franck Bassani:** Writing – review & editing. **Bassem Salem:** Writing – review & editing, Supervision, Methodology, Formal analysis.

Declaration of competing interest

The authors declare that they have no known competing financial interests or personal relationships that could have appeared to influence the work reported in this paper.

Data availability

Data will be made available on request.

Acknowledgment

This work was partly supported by the French RENATECH network through the PTA technological platforms in Grenoble and has received a partial funding from IPCEI/Nano2026.

Appendix A. Supplementary data

Supplementary data to this article can be found online at https://doi.org/10.1016/j.mssp.2024.108851.

References

[1] A. Kaneko, A. Yagishita, K. Yahashi, T. Kubota, M. Omura, K. Matsuo, I. Mizushima, K. Okano, H. Kawasaki, S. Inaba, T. Izumida, T. Kanemura, N. Aoki, K. Ishimaru, H. Ishiuchi, K. Suguro, K. Eguchi, Y. Tsunashima, IEEE Int. Devices Meet. 2005, IEDM Tech. Dig., 2005, pp. 844–847.
[2] F. Koehler, D.H. Triyoso, I. Hussain, B. Antonioli, K. Hempel, Challenges in spacer process development for leading-edge high-K metal gate technology, Phys. Status Solidi C 11 (2014) 73–76.
[3] F. Koehler, D.H. Triyoso, I. Hussain, S. Mutas, H. Bernhardt, Atomic layer deposition of SiN for spacer applications in high-end logic devices, IOP Conf. Ser. Mater. Sci. Eng. 41 (2012) 012006.
[4] J.T. Lin, P.H. Lin, S.W. Haga, Y.C. Wang, D.R. Lu, IEEE Trans. Electron. Dev. 62 (2015) 61–68.
[5] S.Zhang et al Well-suppressed interface states and improved transport properties of AlGaN/GaN MIS-HEMTs with PEALD SiN gate dielectric. Vacuum, ISSN: 0042-207X, Vol: 191, Page: 110359.
[6] M. George Steven, Atomic layer deposition: an overview, Chem. Rev. 110 (2010) 111–131.
[7] Richard W. Johnson, Adam Hultqvist, Stacey F. Bent, A brief review of atomic layer deposition: from fundamentals to applications, Mater. Today 17 (5) (2014) 236–246. ISSN 1369-7021.
[8] Xin Meng, et al., Atomic layer deposition of silicon nitride thin films: a review of recent progress, challenges, and outlooks, Materials 9 (2016) 1007, https://doi.org/10.3390/ma9121007.
[9] S. Morishita, S. Sugahara, M. Matsumura, Atomic-layer chemical-vapor-deposition of silicon-nitride, Appl. Surf. Sci. 112 (1997) 198–204.
[10] K. Park, W.-D. Yun, B.-J. Choi, H.-D. Kim, W.-J. Lee, S.-K. Rha, C.O. Park, Growth studies and characterization of silicon nitride thin films deposited by alternating exposures to Si2Cl6 and NH3, Thin Solid Films 517 (2009) 3975–3978.
[11] S. Riedel, J. Sundqvist, T. Gumprecht, Low temperature deposition of silicon nitride using Si3Cl8, Thin Solid Films 577 (2015) 114–118.
[12] Won-Jun Lee, et al., A comparative study on the Si precursors for the atomic layer deposition of silicon nitride thin films, J. Kor. Phys. Soc. 45 (5) (November 2004) 1352~1355.
[13] aAlain E. Kaloyeros et al Review—Silicon Nitride and Silicon Nitride-Rich Thin Film Technologies: State-of-the-Art Processing Technologies, Properties, and Applications. ECS Journal of Solid State Science and Technology, Volume 9, Number 6. b H.B. Profijt, S.E. Potts, M.C.M. van de Sanden, W.M.M. Kessels, Plasma-assisted atomic layer deposition: basics, opportunities, and challenges, J. Vac. Sci. Technol. A Vacuum, Surfaces, Film. 29 (5) (2011) 050801, https://doi.org/10.1116/1.3609974.
[14] Tahsin Faraz, et al., Atomic layer deposition of wet-etch resistant silicon nitride using di(sec-butylamino)silane and N2 plasma on planar and 3D substrate topographies, ACS Appl. Mater. Interfaces 9 (2) (2017) 1858–1869.
[15] Sejoon Kim Harrison, et al., High growth rate and high wet etch resistance silicon nitride grown by low temperature plasma enhanced atomic layer deposition with a novel silylamine precursor, J. Mater. Chem. C 8 (2020) 13033–13039.
[16] Harm C.M. Knoops, et al., Atomic layer deposition of silicon nitride from bis(tert-butylamino)silane and N2 plasma, ACS Appl. Mater. Interfaces 7 (35) (2015) 19857–19862.
[17] S.W. King, Plasma-enhanced atomic layer deposition of SiN x:H and SiO2, J. Vac. Sci. Technol. 29 (A 2011) 041501.
[18] W. Jang, H. Jeon, C. Kang, H. Song, J. Park, H. Kim, H. Seo, M. Leskela, H. Jeon, Temperature dependence of silicon nitride deposited by remote plasma atomic layer deposition, Phys. Status Solidi A 211 (2014) 2166–2171.
[19] Maxime Legallais, et al., Improvement of AlN film quality using plasma enhanced atomic layer deposition with substrate biasing, ACS Appl. Mater. Interfaces 12 (2020) 39870–39880.
[20] Tahsin Faraz, et al., Energetic ions during plasma-enhanced atomic layer deposition and their role in tailoring material properties, Plasma Sources Sci. Technol. 28 (2019) 024002.
[21] H. Kim, S. Woo, J. Lee, Y. Kim, H. Lee, I.J. Choi, Y.D. Kim, C.W. Chung, H. Jeon, Effect of DC bias on the plasma properties in remote plasma atomic layer deposition and its application to HfO2 thin films, J. Electrochem. Soc. 158 (1) (2011) H21.
[22] H.B. Profijt, M.C.M. van de Sanden, W.M.M. Kessels, Substrate biasing during plasma-assisted ALD for crystalline PhaseControl of TiO2 thin films, Electrochem. Solid State Lett. 15 (2) (2011) G1–G3.
[23] V. Beladiya, T. Faraz, W.M.M. Kessels, A. Tünnermann, A.V. Szeghalmi, Controlling mechanical, structural, and optical properties of Al2O3 thin films

deposited by plasma-enhanced atomic layer deposition with substrate biasing, in: M. Lequime, H.A. Macleod, D. Ristau (Eds.), Advances in Optical Thin Films VI, 2018, p. 13, https://doi.org/10.1117/12.2312516. SPIE.
[24] Vivek Beladiya, et al., Plasma-enhanced atomic layer deposition of HfO2 with substrate biasing: thin films for high-reflective mirrors, ACS Appl. Mater. Interfaces 14 (12) (2022) 14677–14692.
[25] Sean W. King, et al., Plasma enhanced atomic layer deposition of SiNx:H and SiO2, J. Vac. Sci. Technol. A 29 (2011) 041501.
[26] Chaitanya Krishna Ande, et al., Role of surface termination in atomic layer deposition of silicon nitride, J. Phys. Chem. Lett. 6 (2015) 3610–3614.
[27] D.K. Rai, A.K. Panchal, D.S. Sutar, C.S. Solanki, K.R. Balasubramaniam, Mechanism for formation of ultra-thin SiNx on a-Si - XPS and FTIR studies, in: 2015 IEEE 42nd Photovoltaic Specialist Conference (PVSC), 2015, pp. 1–6, https://doi.org/10.1109/PVSC.2015.7355805.
[28] Xianglong Nie, et al., Thermodynamics and kinetic behaviors of thickness-dependent crystallization in high-k thin films deposited by atomic layer deposition, J. Vac. Sci. Technol. A 33 (2015) 01A140.
[29] Shinya Iwashita, et al., Effect of ion energies on the film properties of titanium dioxides synthesized via plasma enhanced atomic layer deposition, J. Vac. Sci. Technol. A 36 (2018) 021515.
[30] Tahsin Faraz, et al., Tuning material properties of oxides and nitrides by substrate biasing during plasma-enhanced atomic layer deposition on planar and 3D substrate topographies, ACS Appl. Mater. Interfaces 10 (15) (2018) 13158–13180.